Chapter 6
Secondary Organic Aerosol Formation from Cyclohexene Ozonolysis: Effect of OH Scavenger and the Role of Radical Chemistry*

* This chapter is reproduced by permission from "Secondary organic aerosol formation from cyclohexene ozonolysis: Effect of OH scavenger and the role of radical chemistry" by M.D. Keywood, J.H. Kroll, V. Varutbangkul, R. Bahreini, R.C. Flagan, J.H. Seinfeld, *Environmental Science and Technology*, 38 (12): 3343-3350, 2004.

6.1. Abstract

In order to isolate secondary organic aerosol (SOA) formation in ozone-alkene systems from the additional influence of hydroxyl (OH) radicals formed in the gas-phase ozone-alkene reaction, OH scavengers are employed. The detailed chemistry associated with three different scavengers (cyclohexane, 2-butanol and CO) is studied in relation to the effects of the scavengers on observed SOA yields in the ozone-cyclohexene system. Our results confirm those of Docherty and Ziemann (*1*) that the OH scavenger plays a role in SOA formation in alkene ozonolysis. The extent and direction of this influence are shown to be dependent on the specific alkene. The main influence of the scavenger arises from its independent production of HO_2 radicals, with CO producing the most HO_2, 2-butanol an intermediate amount, and cyclohexane the least. This work provides evidence for the central role of acylperoxy radicals in SOA formation from the ozonolysis of alkenes and generally underscores the importance of gas-phase radical chemistry beyond the initial ozone-alkene reaction.

6.2. Introduction

Chamber experiments are invaluable for understanding secondary organic aerosol (SOA) formation, with the ability to isolate chemical systems of interest. A trademark system that has received considerable attention is the ozonolysis of cyclohexene. One reason for this is the that the structure of cyclohexene may be viewed as a building block on which many of the more complicated biogenic hydrocarbons are based. In addition, for a number of cyclic alkenes ozonolysis is the major pathway to aerosol formation. It is well established that the OH radical is a by-product of alkene-ozone reactions (*2*). Thus, in order to isolate SOA formation in any alkene-ozone system in chamber experiments it

is necessary to remove OH from the system, via a molecular OH scavenger. Scavengers commonly used in this regard include cyclohexane, CO, alcohol, and aldehydes. Most investigations of ozone-alkene chemistry have had the goal of understanding the yield of OH, and so have been concerned primarily with the effect of the scavenger on the gas-phase chemistry (*2-4*). Recently, it has been suggested that the OH scavenger can have an effect on the SOA yield itself (*1, 5*). For example, in the cyclodecene-ozone system, in the presence of propanol scavenger, Ziemann (*5*) observed the formation of cyclic peroxyhemiacetals, and while these products were not shown explicitly to result in an increase in aerosol yield we may suppose that these large cyclic peroxyhemiacetals partition to the aerosol phase. In contrast to this, Docherty and Ziemann (*1*) observed a reduction in SOA yield for the β-pinene ozonolysis when propanol scavenger was used, compared with cyclohexane as a scavenger.

The reaction between cyclohexene and ozone is initiated by the addition of ozone to the double bond to form a primary ozonide which stabilizes or decomposes to an excited bifunctional Criegee intermediate that has two isomers (*5*) (Figure 6.1). How this intermediate then goes on to form SOA has been discussed extensively (*5, 7-9*). The predominant low molecular weight SOA products identified in the cyclohexene-ozone system are dicarboxylic acids and hydroxylated dicarboxylic acids (*8*). Hydroxyl radicals can be produced from various reactions in the alkene ozonolysis mechanism. The dominant pathway of OH formation is understood to be from the syn isomer of the carbonyl oxide, since the alkyl group in the syn position is able to interact with the terminal oxygen (*10, 11*).

Understanding the chemical role played by the OH scavenger in SOA formation in alkene-ozone systems is important in separating the effects of the scavenger itself from that of the intrinsic ozone-alkene reactions in SOA formation. Moreover, differences in observed SOA yields and products when different scavengers are used provide important clues to the gas-phase chemistry occurring in the system. In the present work we present a detailed analysis of the SOA yields and associated chemistry in the cyclohexene-ozone system when different OH scavengers are used. The differences will be seen to provide key insights into the chemistry leading to SOA formation.

6.3. Experimental Methods

Ozonolysis of cyclohexene in the presence of different OH scavengers (cyclohexane, 2-butanol, and CO) and in the absence of OH scavenger was carried out in the Caltech Indoor Chamber Facility. Details of this facility have been described in detail elsewhere (*12*) and details of the experimental methods employed in these experiments are described in Keywood et al. (*13*). In short, the experiments were carried out in the presence of $(NH_4)_2SO_4$ seed, and the volume of SOA was determined by scanning electrical mobility spectrometers (SEMS). Temperature and RH within the chambers were measured continuously; temperature of operation of the chambers was 20±2 ˚C and the RH was <10%. Concentration of the parent hydrocarbon was determined by gas chromatography flame ionization detection.

The OH scavengers, cyclohexane, 2-butanol, and CO, were injected at sufficient concentration so that the reaction rate of OH radicals with the scavenger exceeded that of the OH with the cycloalkene by a factor of 100. The liquid scavenger compounds were injected into a glass bulb and gently heated as a stream of clean air was passed through

the bulb, vaporizing the scavenger and carrying it into the chamber. Microliter syringes were used to inject known amounts of liquid cyclohexene into the chambers using the same method. The reaction was initiated with the injection of ozone. Ozone was generated using a UV lamp ozone generator, and continuously measured. The total concentration of ozone injected was sufficient to exceed the parent hydrocarbon concentration by a factor of 3.

6.4. Experimental Results

The experiments discussed in this paper are listed in Table 6.1. The table lists the date of the experiment, the concentration of cyclohexene consumed (ΔHC), the identity of the scavenger, the mass concentration of SOA produced (ΔM_o) and the SOA yield (Y). ΔM_o was determined from the change in aerosol volume (measured by the SEMS) and assuming a particle density of 1.4 g cm^{-3}, as determined by Kalberer et al. (*8*) for the cyclohexene-ozone system. Measured particle number concentrations were corrected for size-dependent wall loss (*13*). SOA yield (Y) can be defined as the ratio of organic aerosol mass concentration produced (ΔM_o, μg m^{-3}) to the mass concentration of hydrocarbon consumed (ΔHC, μg m^{-3}), $Y = \Delta M_o / \Delta HC$.

Figure 6.2 shows the SOA yields from the ozonolysis of cyclohexene as a function of aerosol mass produced (ΔM_o) when the different OH scavengers, cyclohexane, 2-butanol, and CO, are used. Also shown are the SOA yields in the absence of scavenger. The data in Figure 6.2 (for cyclohexane and 2-butanol scavengers) are fitted empirically with the two-product model of Odum et al. (*14*), primarily as a convenient way to represent the data. The error bars in Figure 6.2 are computed based on propagation of uncertainties arising in the ΔHC and ΔM_o measurements (*13*).

The use of cyclohexane as an OH scavenger results in the smallest aerosol yield as well as low scatter (or variance) about the fitted yield curve (Figure 6.2). 2-Butanol scavenger results in a higher SOA yield than that of cyclohexane and greater variance about the fitted yield curve. When no scavenger is used, the SOA yield is similar to that when 2-butanol is used; finally, the use of CO as a scavenger results in the greatest yield (as well as the greatest uncertainty in the measurement).

The scatter about the yield curves apparent in Figure 6.2 may be partially attributed to variance in temperature. Temperature affects the vapor pressure of the gaseous secondary products resulting in increased partitioning to the particle phase at lower temperatures and conversely, at higher temperature, reduced partitioning. This effect is clearly demonstrated in Figure 6.3, which shows SOA yield for the ozonolysis of cyclohexene in the presence of 2-butanol scavenger carried out at 30 ºC and 25 ºC, and compares these yields with the data for 20 ºC. As temperature increases, the yield decreases. The extent of deviation of the measured SOA yield from the fitted curve is plotted against temperature in Figure 6.4. A statistically significant linear relationship can be seen between temperature and deviation from the fitted yield curve, suggesting that the scatter about the fitted yield curve may be due to temperature variation. When the yield is corrected for this temperature dependence (Figure 6.5), the data for cyclohexane scavengers all fall completely on the fitted yield curve. For the 2-butanol scavenger, the temperature corrected data in general fall closer to the fitted curve, although some scatter about the curve still exists. While the small variance in the cyclohexane scavenger data can be explained entirely by temperature differences, for the 2-butanol scavenger only a fraction of the variance can be attributed to temperature.

6.5. Scavenger Chemistry

Understanding the reasons for the observed effects of the OH scavenger on aerosol yields provides a clue to the chemistry occurring in the system. One possible explanation lies in reactions of the stabilized Criegee intermediate (SCI) with the scavenger, which could potentially form different low-volatility products. However, in the case of cyclohexene ozonolysis, such reactions probably do not occur to an appreciable extent, as there is very little SCI formed. Criegee intermediates from endocyclic alkenes are formed with more energy than those from exocyclic alkenes, and so are less likely to be stabilized (*15*). Therefore, SCI yields from cyclohexene ozonolysis are very low, measured to be ~3% (*16*). In addition, it is unlikely that the reaction of the Criegee intermediate with CO would form products of lower volatility than those of the Criegee-2-butanol reaction. Therefore, reactions of the scavengers with the Criegee intermediate probably do not affect aerosol yield significantly.

A more likely explanation for the observed effect of the scavenger on SOA yield may lie in the differing radical products formed in the OH-scavenger reactions. Docherty and Ziemann (*1*) show that different scavengers lead to differences in HO_2/RO_2 ratios, which may have an effect on the subsequent radical chemistry. In the case of the CO scavenger, only HO_2 is produced:

$$OH + CO\ (+ O_2) \rightarrow HO_2 + CO_2 \qquad \text{(R12 in Table 6.2)}$$

By contrast, when cyclohexane is used as a scavenger, the radical product is an alkylperoxy radical:

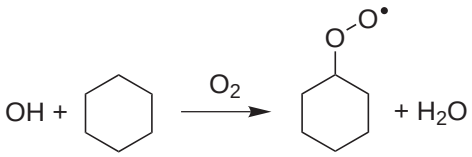

(R19 in Table 6.2)

Some HO_2 production is expected by the OH-cyclohexane reaction due to reactions of the cyclohexylperoxy radical: self-reaction forms an alkoxy radical, which may further react to form HO_2. However, the amount formed is expected to be small. The intermediate case is the reaction of OH with 2-butanol, which may form either HO_2 or RO_2:

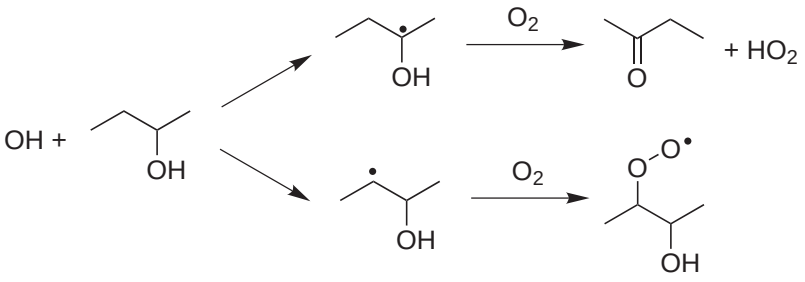

(R13 in Table 6.2)

(The OH radical may abstract hydrogens from the other carbons as well, forming organic peroxy radicals different than the one shown.) Formation of HO_2 is the major channel, with a branching ratio of ~70% (*4*).

The expected trend in the HO_2/RO_2 ratios from each scavenger, CO>2-butanol>cyclohexane, matches that of the aerosol yields, suggesting that increased concentrations of HO_2 and/or decreased concentrations of RO_2, promote aerosol formation. This conclusion is in contrast to that reached by Docherty and Ziemann (*1*), who argue that for β-pinene ozonolysis, increased HO_2/RO_2 ratios instead *inhibit* aerosol formation.

6.6. Mechanism Description

In order to better understand the role that differences in scavenger chemistry may have on the ozonolysis reaction system, and why β-pinene and cyclohexene exhibit opposite trends in SOA formation, we have constructed a simple chemical mechanism describing the gas-phase radical chemistry within the chamber. The reactions, rate constants, and branching ratios in the mechanism are listed in Tables 6.2 and 6.3; here we highlight the important aspects of the mechanism.

The reaction of cyclohexene and ozone (R1) is known to form OH radicals in high yields; we assume a yield of 0.6, based upon three studies (*3, 10, 17*). The vast majority of the OH formed (>95%) undergoes reaction with the scavenger; while some small fraction may react with the parent alkene, we omit this reaction channel. The OH-scavenger reaction (R12, R13, or R19) then produces HO_2 and/or RO_2, as discussed above. In addition, whenever an OH is formed by the ozonolysis reaction, an R radical, which immediately becomes RO_2 in air, is also co-generated. These radicals, the RO_2 from the ozonolysis reaction and the HO_2 and/or RO_2 from the OH-scavenger reaction, are responsible for the ensuing radical chemistry in the chamber. Because the experiments were carried out in the absence of NO_X, the chemistry consists largely of self- and cross-reactions of peroxy species, i.e., HO_2-HO_2, RO_2-RO_2, and HO_2-RO_2. We therefore focus on the evolution of these peroxy radicals, only explicitly following the key molecular compounds, ozone, cyclohexene, scavenger, and organic acids.

The chemistry of most of the individual alkylperoxy species has not been studied in detail, so we represent only three different classes of alkylperoxy radicals, shown in Figure 6.6. The first is formed from the ozonolysis reaction, in yields equal to that of

OH. For cyclohexene ozonolysis, this radical, denoted "RO_2" in the mechanism, has the structure shown in Figure 6.6a. We assume this radical may ultimately react to form the low-volatility products that are incorporated in the SOA.

The structure of RO_2 is similar to that of the acetonoxy radical ($CH_3C(O)CH_2O_2$), which has been extensively studied, so we expect their chemistries to be similar. Reaction with HO_2 (R14) is chain-terminating, leading to the formation of a hydroperoxide; however, reaction with another alkylperoxy may be either chain-terminating (forming an alcohol and a carbonyl) or chain-propagating, forming two alkoxy radicals (RO). The resulting RO is short-lived, and likely reacts either by decomposition or isomerization (Figure 6.7). This branching ratio has not been measured, so we assign the decomposition channel a branching ratio of 0.5, that of a structurally similar species, the β-hydroxyalkoxy radical from OH+1-hexene (*24*). We note that our qualitative results are insensitive to this value. Isomerization mostly occurs by a 1,5-hydrogen shift (R11b), ultimately forming a different alkylperoxy radical, R'O_2. However, RO_2 and R'O_2 are structurally similar, differing by a single OH group, so for simplicity we treat them as the same species. In addition, a 1,6-hydrogen shift to form an acyl radical (which quickly becomes an acylperoxy radical) may also be a minor channel, for which we assign a branching ratio of 0.05. We note that reaction pathways other than those shown above may be available to the RO radical, but these will only make HO_2 or large alkylperoxy radicals, so we assume these pathways are incorporated into the reactions R11a and R11b.

The second class of alkylperoxy radicals represented is that from the reaction of OH with scavengers (cyclohexene and 2-butanol), shown in Figure 6.6b and denoted R^SO_2.

These radicals exhibit similar chemistry to the RO_2 radicals, but are represented separately, as they are not expected to be incorporated directly into the aerosol phase. Rates of self-reaction have been measured for such radicals (*22, 23*); though the branching ratios of their alkoxy radicals (R^SO) are less well-constrained, particularly for those from the 2-butanol scavenger. However, the chemistry of most peroxy radicals is generally dominated by reaction with HO_2 and RO_2 (and not R^SO_2), so that mechanism predictions are relatively insensitive to the rates and branching ratios used for the R^SO_2 reactions.

Shown in Figure 6.6c is the third class of alkylperoxy radical, acylperoxy ($AcylO_2$), formed by reaction R11c. As these radicals are derived from RO_2, they too are expected to eventually lead to low-volatility products and contribute to SOA. We represent them explicitly since their chemistry differs from that of other peroxy radicals. Particularly, the reaction with HO_2 forms organic acids, R'C(O)OH (as well as peracids, R'C(O)OOH), which have significantly lower volatility than other molecular species described by the mechanism. Reaction with RO_2 and R^SO_2 may also form R'C(O)OH; the yield is small (~0.1) for a simple alkylperoxy radical like CH_3O_2 (*18*) but is significantly larger (~0.5) for the acetonoxy radical (*25*); we use these values for R^SO_2 and RO_2, respectively. In addition, self-reaction of small acylperoxy radicals forms R'C(O)O, which decompose rapidly to R' + CO_2. We assume this is also the case for the larger acylperoxy radicals formed in the present reaction system, and treat the resulting peroxy radicals as RO_2.

6.7. Mechanism Predictions

Shown in Figure 6.8 are the predicted and measured ozone and cyclohexene concentrations for the first two hours of reaction. Agreement between mechanism and experiment is good, although in the mechanism it was necessary to increase the ozone production from its nominal value of 4 ppb min^{-1} to 5 ppb min^{-1}; this may be the result of errors in the ozone calibration and/or the ozone-cyclohexene rate constant.

Predicted radical concentrations for all three scavengers are shown in Figure 6.9. In all cases radical concentrations peak at around 40 minutes, corresponding to the maximum in [Ozone]×[Cyclohexene] (the maximum in radical production). As expected, HO_2 concentrations vary greatly with scavenger molecule, being highest for CO and lowest for cyclohexane, with alkylperoxy radical concentrations exhibiting the opposite trend. It should be noted that the trend in alkylperoxy radicals as not simply a result of the differences in R^SO_2 produced from the scavengers; RO_2 also varies, despite being produced at the same rate in each case. Instead the trend is a result of the fast HO_2-RO_2 reaction, which leads to shorter RO_2 lifetimes (and thus lower [RO_2]) when [HO_2] is high. Since $AcylO_2$ is formed by self-reaction of alkylperoxy radicals, $AcylO_2$ concentrations exhibit the same trend as RO_2, being ~3.5 times higher for cyclohexane than for CO.

The trends in radical production displayed in Figure 6.9 are expected to have an effect on SOA formation. Among the classes of molecular products in this simplified reaction mechanism, the least volatile species are the organic acids (and peracids), formed by acylperoxy-HO_2 and acylperoxy-alkylperoxy reactions. More complex chemistry not included in the mechanism may lead to the formation of compounds of even lower volatility. However, since acids are known to be an important component of the aerosol

formed in cyclohexene ozonolysis (*5, 8, 26*), it is reasonable to assume their production is related to aerosol growth. Our purpose is not to explicitly model the total organic acids that will be incorporated into the SOA, or to estimate the individual classes of species such as diacids. Instead, we treat gas-phase organic acid formation as a metric for all low-volatility species produced by reactions of acylperoxy radicals, so that we can understand the formation of such species under different reaction conditions. Such species may include diacyl peroxides, compounds of the form R'C(O)OOC(O)R' which have been observed as very low-volatility components of the aerosol generated in cycloalkene ozonolysis (*9*).

The production of organic acids (including peracids) for each of the three scavengers is shown in Figure 6.10. Most organic acids are formed when cyclohexane is used as the scavenger and the least are formed when CO is used. This is a largely a result of the differences in concentrations of the acylperoxy precursors. The mechanism of acid production for each scavenger is somewhat different: with cyclohexane, most (~90%) organic acid is formed from acylperoxy-alkylperoxy reactions, as $[RO_2]$ is relatively high. With CO this fraction is only ~30%, as the higher HO_2/RO_2 ratio leads to acid production dominated by the fast acylperoxy-HO_2 reaction.

The mechanism predictions would seem to be at odds with our experimental data, in which aerosol yields are highest using CO scavenger, intermediate with 2-butanol, and lowest for cyclohexane. Instead, these predictions are consistent with the differences in aerosol yield from β-pinene ozonolysis using different scavengers, as observed by Docherty and Ziemann (*1*). These calculations are essentially in agreement with their explanation that higher HO_2/RO_2 ratios from OH-scavenger reactions lead to lower-

volatility products and thus lower aerosol yields. We note that this is primarily a result of differences in the concentration of alkylperoxy radicals, the self-reaction of which is necessary to form acylperoxy radicals.

Thus far the mechanism neglects the formation of acylperoxy radicals via the direct decomposition of the Criegee intermediate, suggested by Aschmann et al. (*17*) and Ziemann (*9*) in order to rationalize products observed. Moreover, there is experimental evidence (*27*) that some fraction of anti Criegee decomposes via the "hot acid" channel (*28*) to form an acyl radical and OH:

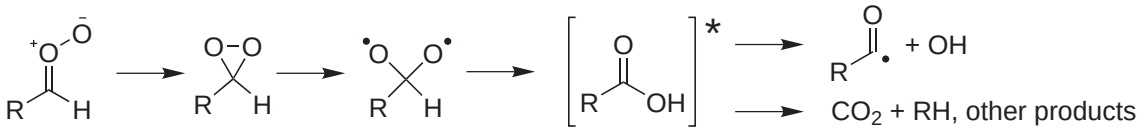

This mechanism of OH formation was shown to be distinct from that shown in Figure 6.6a by the ozonolysis of selectively deuterated 3-hexenes, forming both OH and OD, which were detected separately. While an alternate mechanism involving secondary reactions may have contributed somewhat to OD production (*29*), it is unlikely to have had a large effect, as it cannot account for the large differences in the OD/OH ratios observed for cis and trans alkenes.

Therefore we include the acylperoxy radical as a direct product of the initial ozone-cyclohexene reaction. We assume a yield of 0.05, which is roughly consistent with the results of Kroll et al. (*27*). Even with this relatively low yield, this reaction becomes the dominant source of $AcylO_2$, so that $AcylO_2$ production is no longer limited by alkylperoxy self-reaction. The acylperoxy radical concentration increases by a factor of 3 with the cyclohexane scavenger, and a factor of 10 with the CO scavenger. The difference between the two scavengers arises simply from the fact that [$AcylO_2$] was

greater for the cyclohexene scavenger than for the CO scavenger before the additional acyl source was included in the mechanism (Figure 6.10). These differences have a major effect on the production of organic acids, as shown in Figure 6.11. Including a small source of acylperoxy radicals from the ozonolysis reaction completely reverses the trend in acid production, which is now highest for CO, intermediate for 2-butanol, and lowest for cyclohexene, consistent with our experimental results.

The discrepancy between the observations presented here and those of Docherty and Ziemann (*1*), where SOA yield from the ozonolysis of β-pinene in the presence of cyclohexane were greater than in the presence of propanol, can now be readily explained using the mechanism presented here. Notably, the additional source of acylperoxy radicals does not play a role in the ozonolysis of β-pinene, as the Criegee intermediate formed in that case has no vinylic hydrogens so cannot form acyl radicals via the mechanism shown above. The general mechanism described by this model, in which reactions of acylperoxy radicals are central to aerosol formation, is consistent with both our results and those of Docherty and Ziemann (*1*). The fact that the effect of the scavenger on SOA yields is so much greater for β-pinene than for cyclohexene may be a result of differences in RO_2-RO_2 rate constants. The self-reaction of alkylperoxy radicals is significantly slower when the R group is cyclic (as is the case in β-pinene ozonolysis) than when it is linear (as is the case in cyclohexene ozonolysis), yet RO_2-HO_2 reaction rates are roughly equivalent. Therefore formation of low-volatility products, and thus secondary organic aerosol, is expected to be much more sensitive to HO_2/RO_2 ratios for the ozonolysis of β-pinene than for the ozonolysis of cyclohexene.

We recognize that the ozonolysis reaction mechanism for β-pinene differs from that for cyclohexene in other ways also; for example, the RO radical may decompose to form an acyl radical directly (*1*), leading to higher yields of acylperoxy radicals from the RO_2 self-reaction. However, since we represent general classes of peroxy radicals and not individual species, such mechanistic differences are generally reflected as changes in rate constants and branching ratios, and are not expected to affect our qualitative conclusions significantly.

In cyclohexene ozonolysis in the absence of a radical scavenger, the OH formed will rapidly react with cyclohexene early in the reaction, though as cyclohexene is depleted, OH will begin to react with the reaction products of both cyclohexene-OH and cyclohexene-O_3. Such reactions complicate the gas-phase radical chemistry and may even contribute to aerosol formation, particularly since acyl radicals may be formed in OH-aldehyde reactions. While explicit modeling of the reaction system is beyond the scope of this work, we can, examine the reaction mechanism qualitatively. The peroxy radicals formed by cyclohexene-OH reaction self-react to form β-hydroxyalkoxy radicals, which are expected to decompose only to HO_2, with no RO_2 regeneration or acylperoxy formation (*7*). Thus in the absence of an OH scavenger we expect an HO_2/RO_2 ratio between that of CO and that of cyclohexane, and therefore we expect an aerosol yield between the two. This expectation agrees with our experimental observations.

6.8. Implications

Our results confirm those of Docherty and Ziemann (*1*) that the OH scavenger plays a role in SOA formation during alkene ozonolysis. However, the extent and direction of this influence are dependent on the specific alkene. The main influence of the scavenger

arises from its independent production of HO_2 radicals, with CO producing the most HO_2, 2-butanol an intermediate amount, and cyclohexane producing the least. In the scenario described here, the R^SO_2 radicals produced by the OH scavenger reactions do not participate directly in particle formation; instead, acids are formed by reactions of HO_2-acylperoxy and RO_2-acylperoxy reactions. In the case of β-pinene, where the Criegee intermediate cannot directly form acylperoxy radicals, the presence of high HO_2/RO_2 ratios, as occurs when propanol scavenger is used, results in artificially low SOA levels as the reactions are driven to producing high-volatility products. In the case of cyclohexene, however, acylperoxy radicals are produced by direct decomposition of the Criegee intermediate so the effect of this additional channel has a less significant effect on acid formation for the cyclohexane scavenger than for CO scavenger.

On the surface, the simple reaction scheme of CO with OH makes it an attractive scavenger candidate; however, as shown here, its radical chemistry contributes significantly to SOA yield. Experimentally, CO scavenger resulted in a doubling of the yield relative to cyclohexane. The SOA yields for cyclohexene-ozonolysis presented in Kalberer et al. (*8*) were carried out in the presence of CO scavenger at 25°C and can be compared to the data presented here. As noted above, temperature has a strong effect on SOA yield, so using the simple temperature correction for cyclohexane scavenger shown in Figure 6.4 to correct the Kalberer data to 20°C, again we see an approximate doubling of SOA when CO scavenger is employed, relative to the cyclohexane scavenger data presented here. Additionally, Gao et al. (*26*) present molecular speciation data for the cyclohexane scavenger experiments presented here, and report lower concentrations of hydroxy diacids than reported by Kalberer et al. (*8*). Thus, perturbation to the reaction

mechanism caused by the presence of scavenger related radical productions are seen not only in the total SOA yield but in the composition of the products formed, as expected.

The outcomes presented here suggest that each of the scavengers discussed perturbs SOA yield, since all of the scavenger OH reactions result in the formation of a radical. The ideal scavenger would be one that results in direct chain-termination. This conclusion has implications for the use of SOA yield and molecular speciation data for SOA formation models in atmospheric models. For example, the 2-butanol scavenger data show approximately 30% higher SOA yield than the cyclohexane scavenger data. Docherty and Ziemann (*1*) show 3 times lower yield for the ozonolysis of β-pinene in the presence of propanol scavenger compared with cyclohexane scavenger. The ozonolysis of biogenic hydrocarbons in the presence of 2-butanol scavenger is reported in Griffin et al. (*30*) and Cocker et al. (*31*), and based upon the conclusions reached in this paper, we expect that α-pinene and 3-carene SOA yields are overestimated in those studies, while β-pinene and sabinene are underestimated. However, in order for ozonolysis to be isolated, an OH scavenger must be employed, and until one that results in a chain-termination step can be identified, these scavengers are the most suitable. Highlighted here is the importance of understanding the chemistry of the scavenger itself.

This work has provided more evidence for the central role of acylperoxy radicals in SOA formation in the ozonolysis of alkenes. Only by incorporating these radicals in the chemistry discussed here can the observed trends in SOA formation for the different scavengers be replicated. More generally, this work underscores the importance of radical chemistry beyond the initial ozonolysis reaction steps, and points to the need of a better understanding of the details of such radical-radical reactions.

6.9. Acknowledgment

This research was supported by the Biological and Environmental Research Program (BER), U.S. Department of Energy Grant No. DE-FG03-01ER 63099 and U.S. Environmental Protection Agency Grant RD-831-07501-0. Although the research described in this article has been funded in part by the U.S. Environmental Protection Agency, it has not been subjected to the Agency's required peer and policy review and therefore does not necessarily reflect the views of the Agency and no official endorsement should be inferred.

6.10. References

(1) Docherty, K.S.; Ziemann, P. J. *Aerosol Sci. Tech.* **2003***, 37,* 877.

(2) Paulson, S. E.; Chung, M. Y.; Hassson, A. *J. Phys. Chem. A,* **1999,** *103,* 8125.

(3) Atkinson, R.; Aschmann S. M. *Environ. Sci. Technol.* **1993**, *27*, 1357.

(4) Chew, A.A.; Atkinson R. *J. Geophys. Res.* **1996**, *101*, 28649.

(5) Ziemann, P. J. *J. Phys. Chem. A,* **2003***, 107,* 2048.

(6) Atkinson, R.; Tuazon E. C.; Aschmann S. M., *Environ. Sci. Technol.* **1995**, *29,* 1674.

(7) Calvert, J. G.; Atkinson, R.; Kerr, J. A.; Madronich, S.; Moortgat, G. K.; Wallington, T. J.; Yarwood, G. 2000, The Mechanisms of Atmospheric Oxidation of the Alkenes, Oxford University Press, New York, 552 p.

(8) Kalberer, M.; Yu, J.; Cocker, D. R.; Flagan, R. C.; Seinfeld, J. H. *Environ. Sci. Technol.* **2000**, *34,* 4894.

(9) Ziemann, P. J. *J. Phys. Chem. A,* **2002***, 106,* 4390.

(10) Fenske, J. D.; Kuwata, K. T.; Houk, K. N.; Paulson S. E. *J. Phys. Chem. A*, **2000,** *104,* 7246.

(11) Gutbrod, R.; Meyer, S.; Rahman, M.; Schlinder, R. *Int. J. Chem. Kin*., **1997**, *29*, 717.

(12) Cocker, D. R. III.; Flagan, R. C.; Seinfeld J. H. *Environ. Sci. Technol.* **2001,** *35*, 2594.

(13) Keywood, M. D.; Vartubangkul, V.; Bahreini, R.; Flagan, R. C.; Seinfeld, J. H., *Environ. Sci. Technol.* **2004**, 38, 4157.

(14) Odum, J. R.; Jungkamp, T. P. W; Griffin, R. J.; Flagan, R. C.; Seinfeld, J. H. *Science* **1997***, 276,* 96.

(15) Chuong, B.; Zhang, J.; Donahue, N.M. *J. Am. Chem. Soc.* **2004**, 126, 12363.

(16) Hatakeyama, S.; Kobayashi, H.; and Akimoto. H. *J. Phys. Chem.* **1984**, *88*, 4736.

(17) Aschmann, S. M.; Tuazon, E. C.; Arey, J.; Atkinson R.; *J. Phys. Chem. A*, **2003**, *107*, 2247.

(18) Atkinson, R.; Baulch, D. L.; Cox, R. A.; Crowley, J.; Hampson, R. F.; Jenkin, M. E.; Kerr, J. A.; Rossi, M. J.; Troe, J. Evaluated kinetic and photochemical data for atmospheric chemistry: IUPAC subcommittee on gas kinetic data evaluation for atmospheric chemistry, website url:http://www.iupac-kinetic.ch.cam.ac.uk (accessed Feb 2004).

(19) Atkinson, R. *J. Phys. Chem. Ref. Data*, **1997**, *26,* 215.

(20) Kirchner, F.; Stockwell, W. R. *J. Geophys. Res.* **1996**, *101*, 21007.

(21) Madronich, S.; Calvert, J. D. *J. Geophys. Res.* **1990**, *95*, 5697.

(22) Boyd, A. A.; Lesclaux, R. *Int. J. Chem. Kin.*, **1997**, *29*, 323.

(23) Rowley, D. M.; Lightfoot, P. D.; Lesclaux, R.; Wallington, T. J. *J. Chem. Soc. Faraday Trans.* **1991**, *87*, 3221.

(24) Kwok, E. S. C.; Atkinson, R.; Arey, J.; *Environ. Sci. Technol*. **1996,** *30*, 1048.

(25) Jenkin, M. E.; Cox, R. A.; Emrich, R.; Moortgat, G. K. *J. Chem. Soc. Faraday Trans.* **1993**, *89*, 2983.

(26) Gao, S.; Keywood, M. D.; Ng, N. L.; Surratt, J.; Varutbangkul, V.; Bahreini, R.; Flagan. R. C.; Seinfeld, J. H., *J. Phys. Chem. A* **2004**, 10.1021/jp047466e.

(27) Kroll, J. H.; Donahue, N. M.; Cee, V. J.; Demerjian, K. L.; Anderson, J. G. *J. Am. Chem. Soc.* **2002**, *124*, 8518.

(28) Herron, J. T; Huie, R. E. *J. Am. Chem. Soc.* **1977**, *99*, 5430.

(29) Kuwata, K. T.; Ternpleton, K. L.; Hasson, A. S. *J. Phys. Chem. A*, **2003**, *107*, 11525.

(30) Griffin, R. J; Cocker III, D. R; Flagan, R. C.; Seinfeld, J. H. *J. Geophys. Res.* **1999**, *104***,** 3555.

(31) Cocker III, D. R.; Clegg, S. L.; Flagan, R. C.; Seinfeld, J. H. *Atmos. Environ*. **2001**, *35*, 6049.

Table 6.1. Initial conditions and data for cyclohexene ozonolysis reactions

Date	*Scavenger*	*T °C*	*Cyclohexene (ppb)*	*ΔM_o ($\mu g\ m^{-3}$)*	*Yield*
04/18/02	2-butanol	19.8	90	55	0.196
04/26/02	2-butanol	18.8	51	24	0.141
04/30/02	2-butanol	19.6	54	28	0.153
05/06/02	2-butanol	20.9	102	52	0.156
06/29/02	2-butanol	21.7	86	44	0.152
09/16/02	2-butanol	20.3	263	198	0.224
09/27/02	2-butanol	20.0	241	161	0.203
09/27/02	2-butanol	19.6	57	11	0.057
10/28/02	2-butanol	20.9	271	176	0.194
02/21/03	2-butanol	20.2	291	203	0.208
03/01/03	2-butanol	18.8	262	193	0.216
09/23/02	2-butanol	29.6	60	3	0.018
09/25/02	2-butanol	25.7	112	27	0.073
09/25/02	2-butanol	24.2	240	69	0.094
09/21/02	2-butanol	31.5	227	42	0.059
09/23/02	2-butanol	30.4	82	13	0.051
01/27/03	Cyclohexane	19.3	206	111	0.158
01/29/03	Cyclohexane	20.5	240	101	0.141
02/06/03	Cyclohexane	19.3	119	45	0.111
02/08/03	Cyclohexane	19.2	59	14	0.072
02/10/03	Cyclohexane	19.4	173	81	0.136
03/03/03	Cyclohexane	18.9	81	25	0.090
03/05/03	Cyclohexane	19.8	324	232	0.209
06/04/03	Cyclohexane	19.2	313	200	0.187
02/19/03	No scavenger	19.1	229	165	0.211
02/27/03	No scavenger	19.3	211	141	0.196
11/01/02	No scavenger	21.1	217	146	0.205
11/01/02	CO	20.4	232	180	0.244

Table 6.2. Reactions and rate constants used in the mechanism

No.	*Reaction*			*Rate* [a]	*Note*
R1	Cyclohexene + O_3 *(+* O_2*)*	→	0.6 OH + 0.6 RO_2 + other products	8.1e-17	b
R2	HO_2 + HO_2	→	H_2O_2 + O_2	2.8e-12	c
R3	HO_2 + OH	→	H_2O + O_2	1.1e-10	c
R4	HO_2 + O_3	→	OH + 2 O_2	2e-15	c
R5	OH + O_3	→	HO_2 + O_2	7.3e-14	c
R6	RO_2 + HO_2	→	ROOH + O_2	1.5e-11	d
R7	$AcylO_2$ + HO_2	→	products (see table 6.4)	1.5e-11	d
R8	RO_2 + RO_2	→	products (see table 6.4)	1.4e-12	e
R9	$AcylO_2$ + $AcylO_2$	→	R'C(O)O + R'C(O)O + O_2	1.6e-11	f,g
R10	RO_2 + $AcylO_2$	→	products (see table 6.4)	9.5e-12	h
R11	RO (+ O_2)	→	products (see table 6.4)	rapid	i
	CO scavenger				
R12	OH + CO (+ O_2)	→	HO_2 + CO_2	2.8e-12	c
	2-Butanol scavenger				
R13	OH + 2-butanol (+ O_2)	→	HO_2 + MEK + H_2O	6.4e-12	j
		→	R^SO_2 + H_2O	2.8e-12	j
R14	R^SO_2 + HO_2	→	R^SOOH + O_2	1.5e-11	d
R15	R^SO_2 + R^SO_2	→	products (see table 6.4)	6.7e-13	k
R16	R^SO_2 + RO_2	→	products (see table 6.4)	1.9e-12	h
R17	R^SO_2 + $AcylO_2$	→	products (see table 6.4)	6.5e-12	h
R18	R^SO (+ O_2)	→	products (see table 6.4)	rapid	i
	Cyclohexane scavenger				
R19	OH + cyclohexane (+ O_2)	→	R^SO_2 + H_2O	7.2e-12	l
R14	R^SO_2 + HO_2	→	R^SOOH + O_2	1.5e-11	d
R15	R^SO_2 + R^SO_2	→	products (see table 6.4)	2.8e-14	m
R16	R^SO_2 + RO_2	→	products (see table 6.4)	4.0e-13	h
R17	R^SO_2 + $AcylO_2$	→	products (see table 6.4)	1.3e-12	h
R18	R^SO (+ O_2)	→	products (see table 6.4)	rapid	i

a) All rates in cm^3 $molecule^{-1}$ s^{-1}
b) Reference (*7*); see text for additional products
c) Reference (*18*)
d) For simplicity, all HO_2-RO_2 reactions were assumed to have a rate of 1.5e-11 cm^3 $molecule^{-1}$ s^{-1}, as recommended by Reference (*19*)
e) From parameterization of Reference (*20*)
f) Based on recommendation by Atkinson et al (*18*) for the acetylperoxy radical
g) The R'C(O)O radicals are assumed to decompose to R' + CO_2; R' is then treated as RO_2
h) Following Madronich and Calvert (*21*), rates of all cross peroxy radical reactions are assumed to be twice the geometric mean of the self reaction of the individual peroxy radicals.
i) RO radicals have lifetimes of <20 μs at 1 atm air and so are not explicitly treated in this model.
j) Reference (*4*)
k) Reference (*22*)
l) Reference (*19*)
m) Reference (*23*)

Table 6.3. Branching ratios used in the mechanism

No.	*Reaction*			*Branching Ratio*	*Note*
R7a	$AcylO_2 + HO_2$	→	$R'C(O)OH + O_3$	0.2	f
R7b		→	$R'C(O)OOH + O_2$	0.8	
R8a	$RO_2 + RO_2$	→	$RO + RO + O_2$	0.25	n
R8b		→	carbonyl + ROH	0.75	
R10a	$RO_2 + AcylO_2$	→	$RO + R'C(O)O$	0.5	g,n
R10b			carbonyl + $R'C(O)OH$	0.5	
R11a	$RO (+ O_2)$	→	HO_2 + carbonyl	0.5	o
R11b		→	RO_2	0.45	
R11c		→	$AcylO_2$	0.05	
R15	$R^SO_2 + R^SO_2$	→	$R^SO + R^SO + O_2$	0.3	p
R15b		→	carbonyl + R^SOH	0.7	
R16	$R^SO_2 + RO_2$	→	$RO + R^SO + O_2$	0.5	q
R16b		→	carbonyl + alcohol	0.5	
R17a	$R^SO_2 + AcylO_2$	→	$R^SO + R'C(O)O + O_2$	0.9	g,r
R17b		→	carbonyl + $R'C(O)OH$	0.1	
R18a	$R^SO (+ O_2)$	→	HO_2 + carbonyl	0.5	p
R18b		→	RO_2	0.5	

n) Based upon recommendation by Atkinson et al. (*18*) for $CH_3C(O)CH_2O_2$
o) See text
p) As measured by Rowley et al. (*23*) for the cyclohexylperoxy radical; assumed to be the same for the peroxy radicals formed by OH+2-butanol. Results are relatively insensitive to these parameters.
q) Arbitrary; results are relatively insensitive to this parameter
r) Based upon recommendation by Atkinson et al. (*18*) for CH_3O_2

Figure 6.1. Initial steps of the cyclohexene-ozone reaction

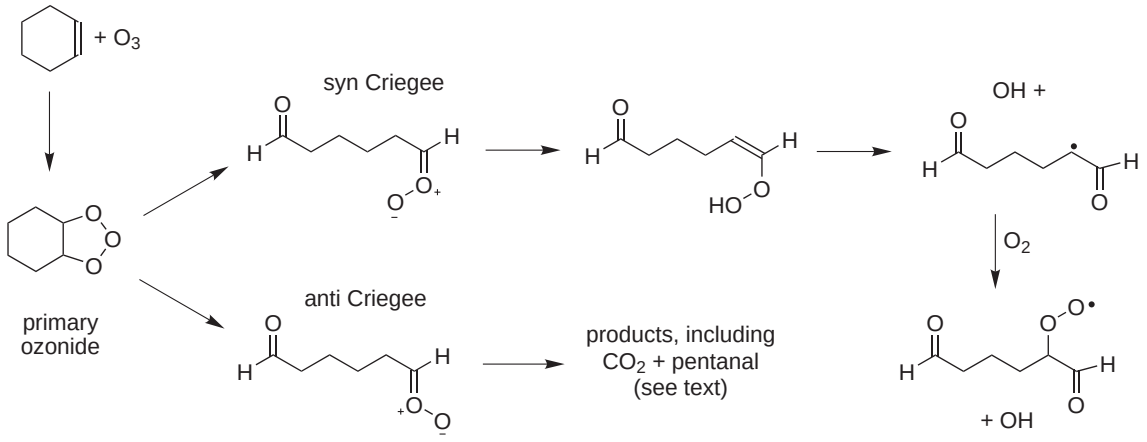

Figure 6.2. SOA yield for ozonolysis of cyclohexene in the presence of different OH scavengers. The two lines are the result of the two-product model used to fit curves to the 2-butanol and cyclohexane scavenger data.

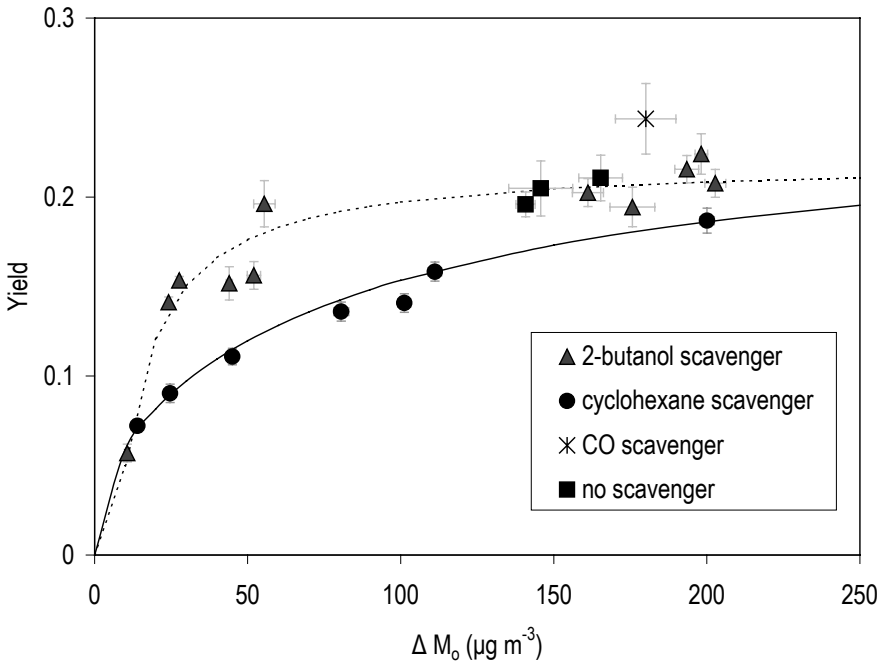

Figure 6.3. SOA yield for ozonolysis of cyclohexene in the presence of 2-butanol at differing temperatures

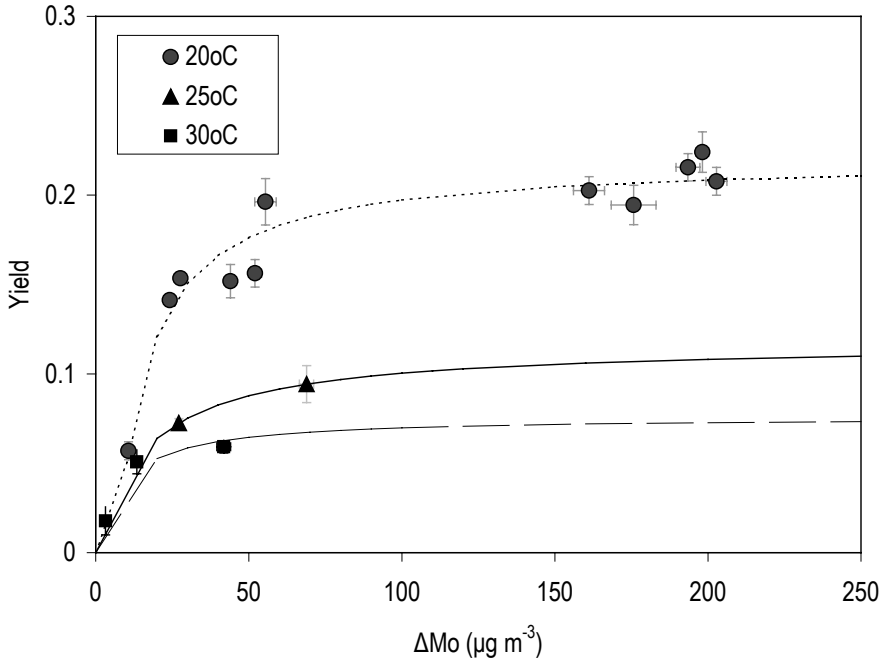

Figure 6.4. Relationship between temperature and deviation in yield from the fitted yield curve for cyclohexane and 2-butanol scavenger experiments

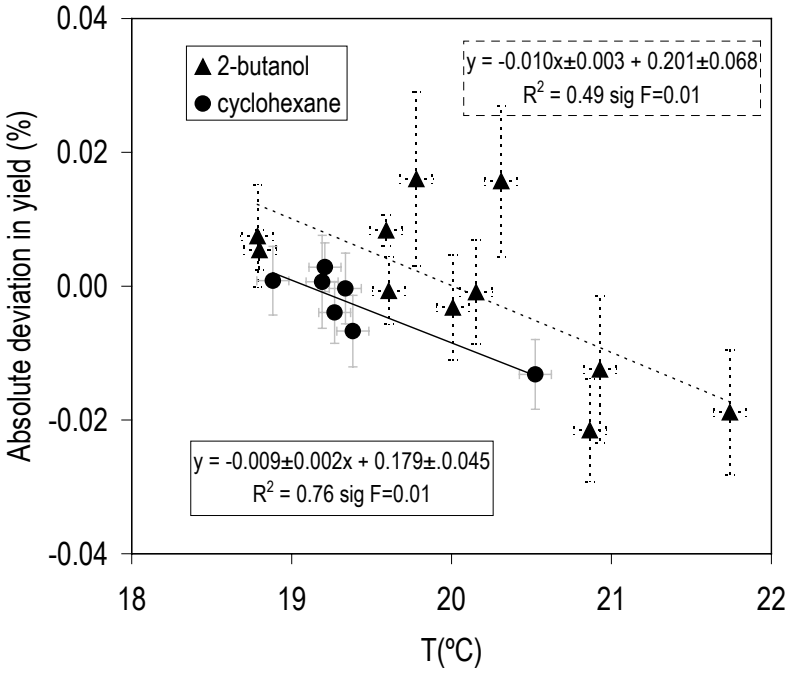

Figure 6.5. SOA yield curves for ozonolysis of cyclohexene in the presence of 2-butanol scavenger and cyclohexane scavengers corrected for temperature variations using the linear relationships displayed in Figure 6.4

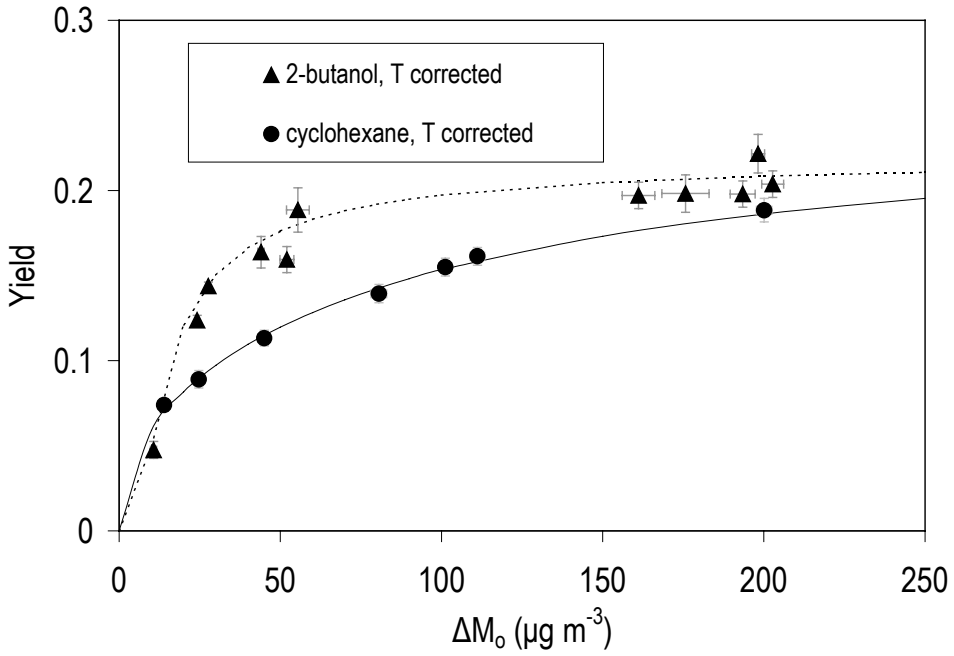

Figure 6.6. The three classes of organic peroxy radicals modeled in this study: (a) RO_2, the peroxy radical co-generated with OH in the ozonolysis reaction; (b) R^SO_2, from reaction with the cyclohexane 2-butanol scavengers; and (c) $AcylO_2$, acylperoxy radicals

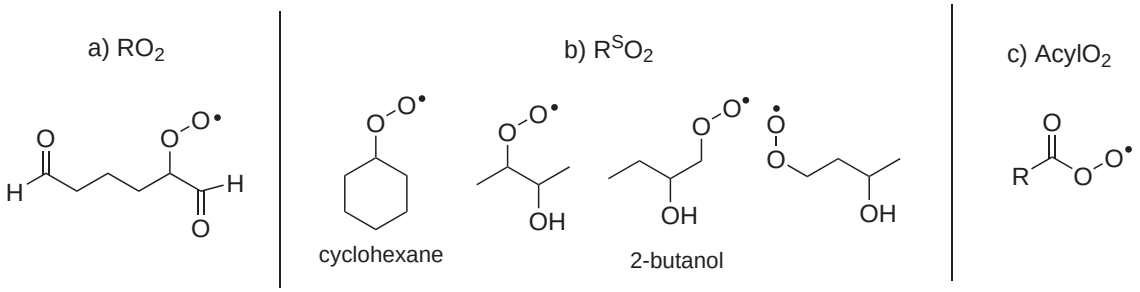

Figure 6.7. Possible reaction pathways of the RO radical generated in the self-reaction of RO_2. Pathways shown are decomposition to form HO_2, isomerization to regenerate RO_2, and isomerization to form $AcylO_2$.

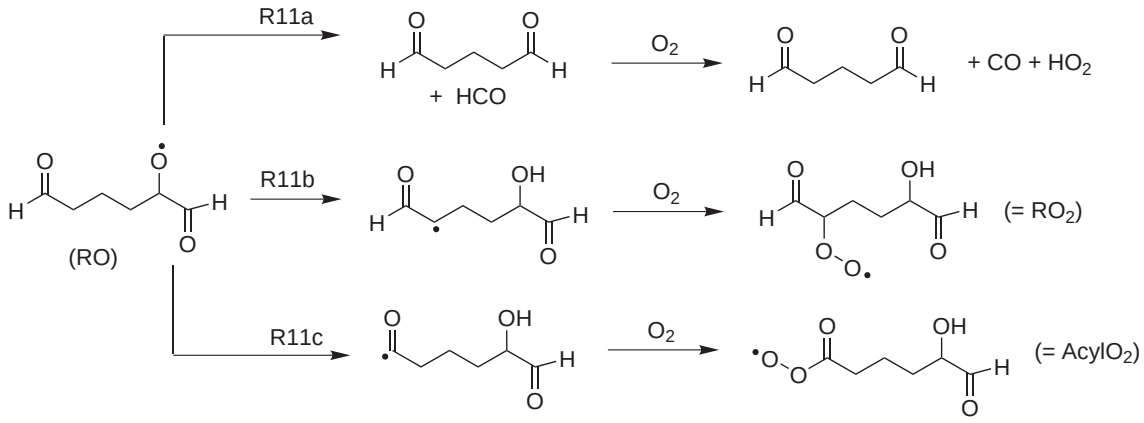

Figure 6.8. Predicted and measured ozone and cyclohexene concentrations for a typical experiment (01/30/03). The straight line indicates predicted ozone concentration if no alkene were present.

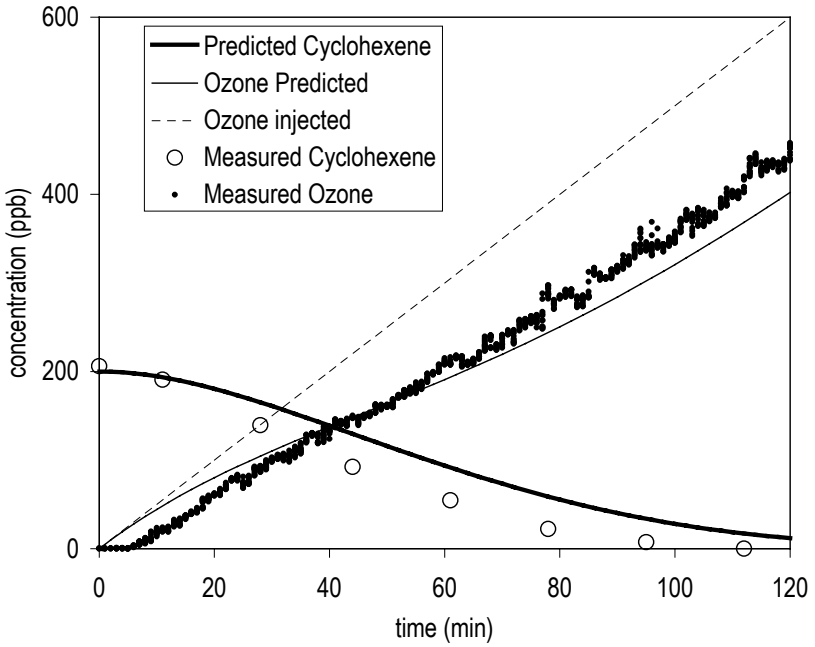

Figure 6.9. Predicted radical concentrations for ozonolysis of 200 ppb of cyclohexene for each of the three scavengers used: (a) CO, (b) 2-butanol, and (c) cyclohexane. Note that for HO_2 and $AcylO_2$ the scale has been expanded by a factor of 100.

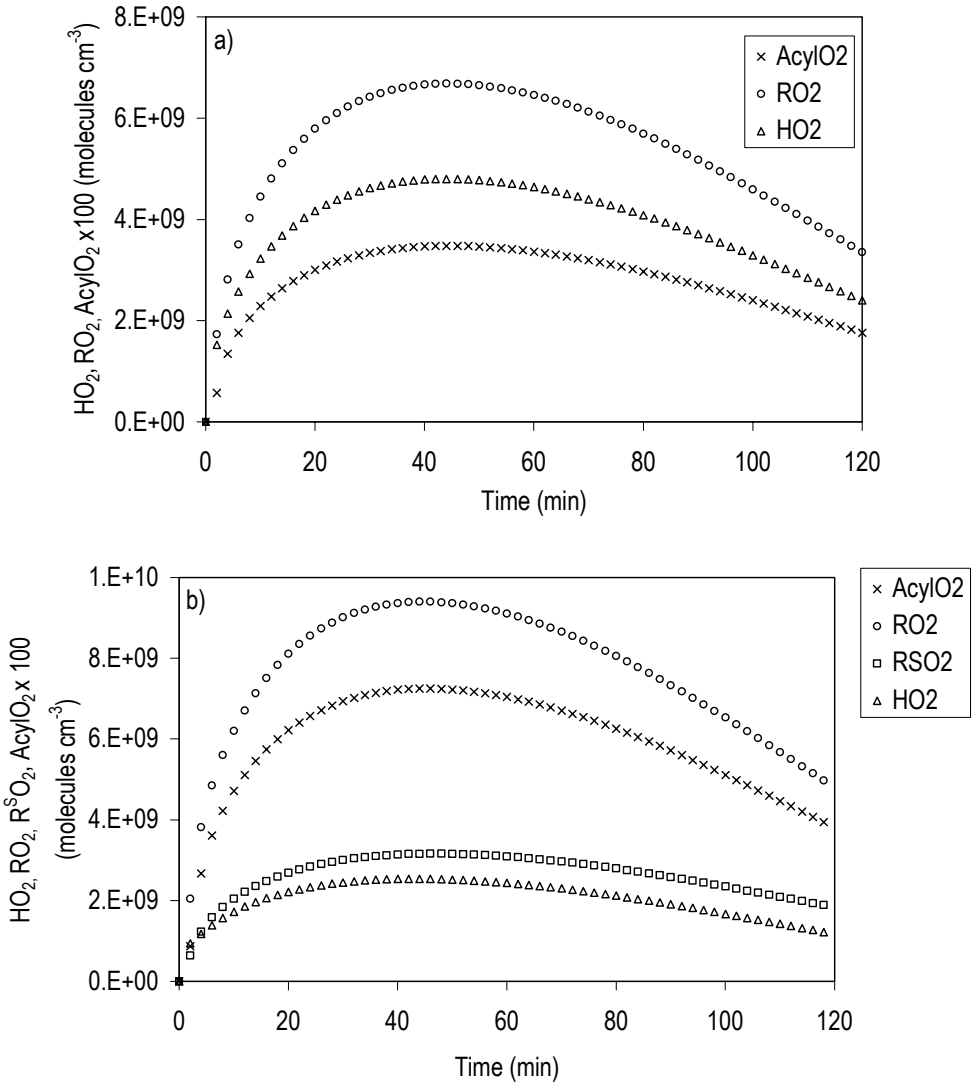

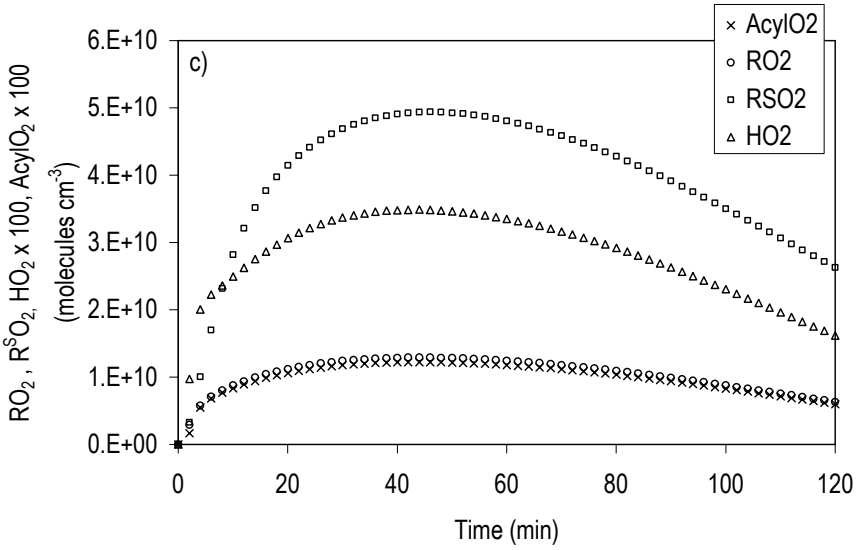
c)
AcylO2
RO2
RSO2
HO2
6.E+10
5.E+10
4.E+10
3.E+10
2.E+10
1.E+10
0.E+00
0
20
40
60
80
100
120
Time (min)
RO2, RSO2, HO2 x 100, AcylO2 x 100
(molecules cm-3)

Figure 6.10. Predicted organic acid (including peracid) concentrations for each scavenger, from the ozonolysis of 200 ppb of cyclohexene, assuming no acyl radicals are formed directly by the ozonolysis reaction

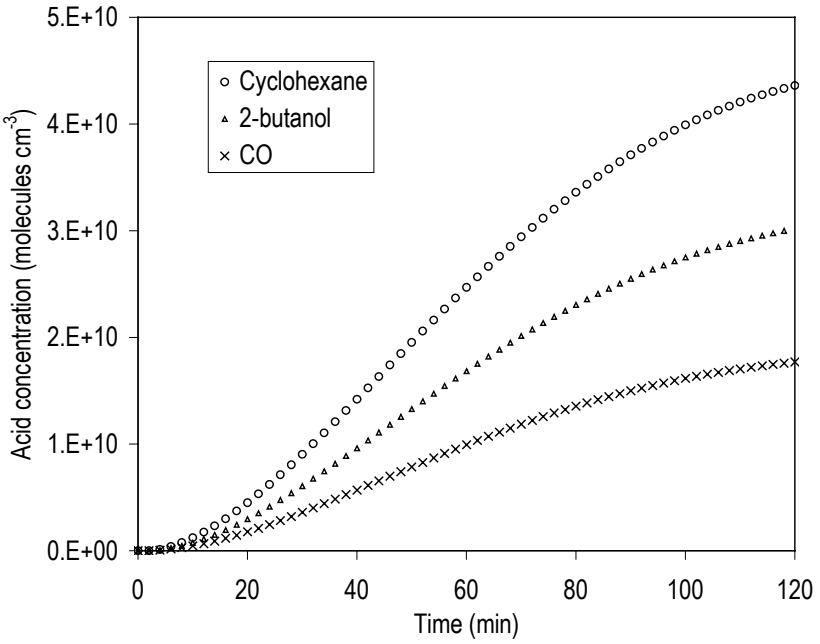

Figure 6.11. Predicted organic acid (including peracid) concentrations for each scavenger, for the ozonolysis of 200 ppb cyclohexene, assuming an acyl radical yield of 0.05 from the ozonolysis reaction